# Combined-Accelerated Stress Testing System for Photovoltaic Modules

Spataru, Sergiu; Hacke, Peter; Owen-Bellini, Michael

*Published in:*
Proceedings of the 2018 IEEE 7th World Conference on Photovoltaic Energy Conversion

*DOI (link to publication from Publisher):*
10.1109/PVSC.2018.8547335

*Publication date:*
2018

*Document Version*
Accepted author manuscript, peer reviewed version

# Combined-Accelerated Stress Testing System for Photovoltaic Modules

Sergiu Spataru,[1] Peter Hacke,[2] Michael Owen-Bellini[2]

[1]Aalborg University, Aalborg, 9220, Denmark
[2]National Renewable Energy Laboratory, Golden, CO 80401, United States

***Abstract* — Combining the stress factors of the natural environment into a single test for photovoltaic modules requires fewer modules, fewer parallel tests, and makes it possible to discover potential weaknesses that are not known *a priori* in new module designs. In this work, we present the necessary *hardware* and *software* capabilities for developing, implementing, and performing Combined-Accelerated Stress Testing (C-AST) protocols for photovoltaic modules, using off-the-shelf equipment and accessible software development tools, with the aim of supporting the development of C-AST capabilities by the photovoltaic community.**

***Index Terms* — photovoltaic modules, acceleration factor, prediction, degradation, combined accelerated stress testing.**

## I. Introduction

Photovoltaic (PV) modules have an expected service life of 25 years or more, whereas the development cycle of new PV module designs can be under a half year [1]. This poses a challenge for module manufacturers, who need to design cost-effective and reliable modules, as well as for investors, who are quantifying and managing risk associated with unexpected failures and degradation, especially for new module designs [2]. Presently, numerous failure mechanisms seen in the field are not screened in existing safety and design qualification tests, and there is no capability to project overall module field durability [3].

In recent years, several *mechanism-specific tests* [2] have been developed, as part of the Qualification Plus Testing [4], as well as *sequential stress testing* procedures [5], that are based on the occurrence, rates, and theory of some of the known failure mechanisms. Such tests are useful for evaluating PV module/material durability to known and dominating stress factors. These require numerous modules and multiple parallel tests to cover most of the known failure mechanisms. However, field results have shown that the combinations of stress factors of the natural environment have markedly greater impact than separate, factor-specific laboratory tests.

A possible solution is *combining the stress factors* of the natural environment: humidity, temperature, light, rain, wind/snow loads, as well as voltage stress, into a single Combined-Accelerated Stress Test (C-AST) for PV modules. This will require fewer modules, and with fewer parallel tests, it will be possible to discover potential weaknesses that are not known *a priori* in new or changed module designs.

With hundreds of gigawatts of PV anticipated to be installed on a yearly basis in the coming years, improved testing that can succeed at reducing cost of risk (financing and insurance) by even tens of basis points can yield great cost savings for this billion-dollar industry.

This work focuses on developing the necessary *hardware* and *software* capabilities for C-AST on PV modules, based on off-the-shelf equipment and accessible software development tools and methods. The overarching goal of this research is to develop a C-AST protocol that is accessible for adoption and implementation in PV testing laboratories across the world.

## II. Combined-Accelerated Stress Testing

The aim of C-AST is to demonstrate—in a single test—degradation processes including (but not limited to) electrochemical corrosion of cell, frame, and grounding parts, delamination, potential-induced degradation (PID), discoloration, backsheet cracking, oxidation of polymeric materials, light-induced degradation, thermomechanical fatigue, failure associated with thermal expansion and elasticity mismatch, solder or electrically conductive adhesive bond failure, edge seal rupture, crack growth in cells, metal migration, and failures of module-integrated electronics and connectors.

The starting point for developing the C-AST methodology and protocol are the ASTM G155 and ASTM D7869, shown in Table I, developed by the automotive and aerospace industries for vehicle film coatings. These protocols specify stress cycle periods for moisture uptake with water spray, irradiance ramps, and light/dark sub-cycles producing thermal shock. A feature of the ASTM D7869 is that the stress levels applied do not exceed those that can be found in the natural environment; thus, artifacts of excessive stress levels found in some accelerated test are mitigated. However, temperature of the modules in this work are raised to 90°C under light to approach temperatures that are measured on some roof-mounted modules.

TABLE I. ASTM D7869 Test Cycle Protocol

| Step no. | Step duration [min] | Function | Irrad. @ 340 nm [W/m²/nm] | Black panel temp. [°C] | Air temp. [°C] | R.H. [%] |
|---|---|---|---|---|---|---|
| 1 | 240 | Dark+spray | – | – | 40 | 95 |
| 2 | 30 | Light | 0.4 | 50 | 42 | 50 |
| 3 | 270 | Light | 0.8 | 70 | 50 | 50 |
| 4 | 30 | Light | 0.4 | 50 | 42 | 50 |
| 5 | 150 | Dark+spray | – | – | 40 | 95 |
| 6 | 30 | Dark+spray | – | – | 40 | 95 |
| 7 | 20 | Light | 0.4 | 50 | 42 | 50 |
| 8 | 120 | Light | 0.8 | 70 | 50 | 50 |
| 9 | 10 | Dark | – | – | 40 | 50 |
| 10 | Repeat steps 6–9 an additional 3 times (for a total of 24 hours) | | | | | |

TABLE II. EXAMPLE OF 24-HOUR PV MODULE COMBINED STRESS TESTING PROTOCOL BASED ON THE ASTM D7869 TEST PROTOCOL

| Step no. | Step Duration [min] | Function(s) | Irradiance [W/m²] | Chamber T setpoint [°C] | Chamber RH setpoint [%] | Water Spray Cycling | Mech. Pressure Cycling | High Voltage |
|---|---|---|---|---|---|---|---|---|
| 1 | 240 | Dark + Spray | – | 40 | 95 | On | – | – |
| 2 | 30 | Light + HV | 800 | 42 | 40 | – | – | On |
| 3 | 267.5 | Light + HV | 1920 | 54 | 30 | – | – | On |
| 4 | 2,5 | Light + HV+ M. Press. | 1920 | 54 | 30 | – | On | On |
| 5a* | 30 | Light + HV | 800 | 42 | 50 | – | – | On |
| 6a* | 100 | Dark + Spray | – | 40 | 95 | On | – | – |
| 7a* | 77 | Dark + Freeze | – | -20 | 0 | – | – | – |
| 8,9a* | 3 | Dark + Freeze + M. Press. | – | -20 | 0 | – | On | – |
| 5b* | 30 | Dark + Dry | – | 20 | 3 | – | – | – |
| 6b* | 60 | Dark + Freeze | – | -20 | 0 | – | – | – |
| 7b* | 3 | Dark + Freeze + M. Press. | – | -20 | 0 | – | On | – |
| 8b* | 30 | Light + Dry + HV | 800 | 40 | 3 | – | – | On |
| 9b* | 90 | Dark + Spray | – | 40 | 95 | On | – | – |
| 10 | 20 | Light + HV | 800 | 62 | 20 | – | – | On |
| 11 | 120 | Light + HV | 1920 | 54 | 30 | – | – | On |
| 12 | 20 | Dark + Spray | – | 40 | 95 | On | – | – |
| 13 | 20 | Dark + Humid | – | 40 | 95 | – | – | – |
| 14 | 20 | Light + HV | 800 | 42 | 40 | – | – | On |
| 15–17 | 160 | Repeat steps 11 to 13 | | | | | | |
| 18–21 | 180 | Repeat steps 14 to 17 | | | | | | |
| 22–23 | 140 | Repeat steps 14 to 15 | | | | | | |
| 24 | 10 | Dark | – | 40 | 50 | | | |

* Phase a (steps 5a–9a) and Phase b (steps 5b–9b) are alternated each day to simulate humid-freeze and dry-freeze stress cycles.

Compared to the ASTM D7869 shown in Table I, the new C-AST protocol will additionally need to:

- Include effects of freezing
- Include voltage-bias stress to simulate the module's voltage potential in series strings (only during light conditions)
- Include mechanical stress to simulate snow or wind loads.

Based on these considerations, a preliminary C-AST protocol for PV modules, shown in Table II, is being tested and fine-tuned together with the C-AST chamber for a module backsheet degradation study. Preliminary test results are presented in section V of this paper, and more details and results regarding the application of the C-AST protocol will be published in a future paper [6].

## III. HARDWARE IMPLEMENTATION

From a practical perspective, developing a C-AST testing system, capable of performing tests such as the one proposed in Table II, requires the ability to control and monitor a number of process variables, summarized in Table III. Based on these requirements, the necessary hardware subsystems have been designed and selected and are described next.

TABLE III. OVERVIEW OF C-AST PROCESS VARIABLES

| Controlled Variables | Monitored Variables |
|---|---|
| Ambient temperature | |
| | Module temperature |
| Ambient relative humidity | |
| Rain (water spray) | |
| Module voltage bias | |
| | Module leakage current |
| Mechanical pressure | |
| | Module mech. press. response |
| Irradiance @ 340 nm | |
| | Global irradiance |
| | Module power |
| | Module voltage |
| | Module current |

The main hardware components of the C-AST system for controlling different stress factors and monitoring the module degradation are shown in Fig. 1.

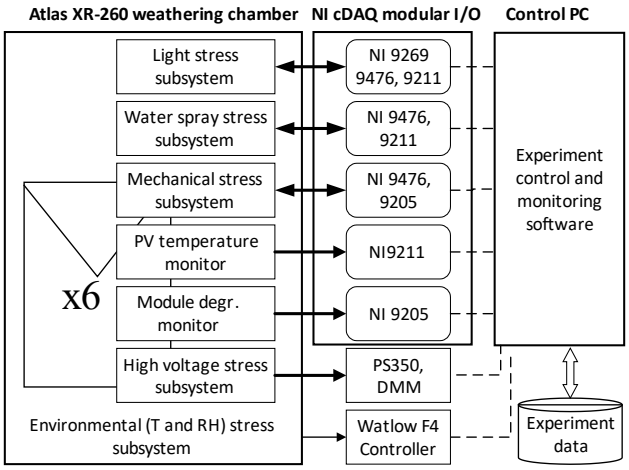


Fig. 1. Overview of C-AST hardware subsystems.

*A. Environmental Stress Subsystem*

The **Environmental Stress Subsystem** consists of an Atlas XR-260 weathering chamber, shown in Fig. 2, with a test plane of 1.2 m × 1.8 m that is presently facilitated for six 4-cell mini-modules and eventually eight such modules, or larger modules of differing designs. The internal chamber air temperature (T) and relative humidity (RH) can be regulated between -40°C and 95°C, and between 5% and greater than 95%, respectively, by means of a Watlow F4 controller. The digital controller allows programmatic remote control and monitoring of the chamber temperature and humidity test profiles, through a serial RS232 interface.

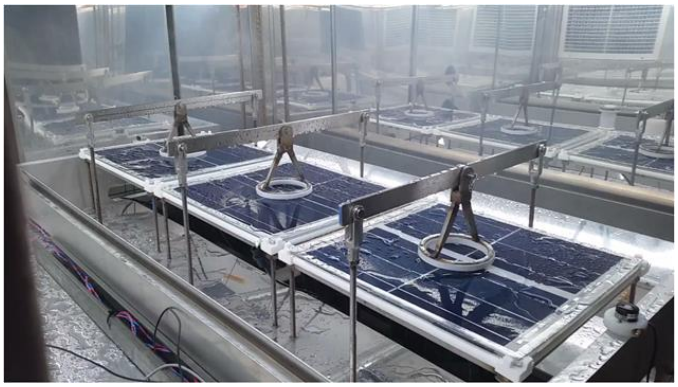

Fig. 2. Inside view of chamber and mini-modules.

*B. Light Stress Subsystem*

The **Light Stress Subsystem** consists of four water-cooled xenon arc lamps, mounted about 0.8 m above the test plane, installed with a reflector system. The lamps are spectrally filtered to simulate solar irradiance with a light spectrum matching AM 1.5 in the ultraviolet (UV) and visible light ranges. In addition, troughs are installed on the test plane to simulate ground albedo and to reflect ~10% of incoming UV light toward the module backsheet.

The four xenon arc lamps are driven by an AC signal and they generate an irradiance that varies over time. This poses a limitation for accurately simulating PV module stress factors that are light-dependent, such as high-voltage stress and PID, which are only present under light conditions.

Four white-light LED strings (Superbrightleds 4NFLS-CWH12960-24V), have been installed in the chamber to generate a minimum level of light bias, equivalent to ~50 W/m$^2$ on the module plane so that voltage over the cell junctions in the modules and application of system voltage stress can be maintained in a field-representative condition during periods when the Xe light is off.

The operation of the Xe lamps and LED strings is controlled on two levels. First, the power supply to the lamps and LEDs is connected/disconnected through a bank of solid-state relays that are controlled by a National Instruments (NI) 9476 Digital Output (DO) card. Second, the intensity of each lamp and LED is controlled by an analogue reference signal, digital-to-analogue converter (DAC) card NI 9269, which is part of a modular Compact DAQ system from NI.

It is well known that material degradation due to light exposure is mainly caused by the UV band of the light spectrum [7], and it is the main light stress factor that must be controlled during testing. However, the UV properties of Xe lamps change over time due to ageing, and their intensity must be adjusted to generate a constant UV stress. To achieve this, four spectrally filtered (340-nm) light-pipe photodiodes integral to the chamber were used to control and adjust the Xe light intensity. In addition, two total UV radiometers (TUVRs) are used to monitor the UV band and ageing of the Xe lamps.

To monitor the total solar irradiation in the chamber and characterize the performance of the mini-modules, six LICOR pyranometers (LI-61713) were installed on the test plane.

The light pipes, LICORs, TUVRs sensors, as well as LED and TUVR temperatures are measured using NI 9211 analogue-to-digital converter (ADC) cards with a sampling rate of 0.5 Hz, used to regulate chamber light with control feedback loop. Additionally, the LICORs and TUVRs are sampled at 2 kHz with a NI 9205 card for referencing PV module performance.

*C. Water-Spray Stress Subsystem*

The **Water-Spray Stress Subsystem** built into the Atlas XR-260 chamber can simulate condensing humidity/rain cycles by a simple solenoid and electric valve. The system is equipped with a water preheater and a water temperature sensor for controlling water-spray temperature during testing. The spray is introduced to the chamber at a programmed pulse frequency and duty cycle both from the module faces and rears.

*D. Mechanical Stress Subsystem*

The **Mechanical Stress Subsystem** for applying dynamic mechanical load cycles to the test modules consists of hydraulic actuators applying pressure to the module face with 100-mm-diameter steel “donuts” enveloped in Teflon, mechanical

pressure valve and mechanical stop, for controlling the displacement and adjusting the pressure applied to the module. Desired pressure is achieved by calculating and/or measuring the required displacement to achieve that pressure.

Cyclic dynamic mechanical loading of 1,000 Pa required by IEC Technical Specification 62782 is translated to a displacement of 1.1 mm at the center of the mini-module; however, a more rigorous analysis to improve the replication of the stress state in full-size modules is being performed. About 1,000 cycles per month are applied on the light-facing side to simulate a snow or wind load.

The mechanical loading is controlled in an on/off manner by a NI 9476 DO card. The transient pressure/loading response of the test modules is measured with a pressure sensor and fast NI 9205 ADC card for detecting changes and mechanical failure events in the modules.

### *E. High-Voltage Stress Subsystem*

The **High-Voltage Stress Subsystem** consists of two Stanford PS 350 high-voltage (HV) power supplies—one configured for applying positive and one for negative HV—between the module leads and frame. Module leakage current (LC) is monitored on the HV side of each PV module because the module surface and frame get wet during the testing, and there is no practical way to isolate the modules. The LC of each of the test modules is measured with a Keithley 2700 digital multimeter (DMM). It is important to mention that this solution is not optimal because the DMM can only provide isolation up to 500 V. In the future, the DMM will be replaced with a completely isolated voltage meter capable of operating up to 1,500 V.

### *F. PV Module Temperature Monitoring Subsystem*

The **PV Module Temperature Monitoring Subsystem** consists of two temperature sensors mounted on each test module (12 in total), and three NI 9211 ADC cards with a sampling rate of 0.5 Hz.

### *G. In-Situ Module Degradation Monitoring Subsystem*

The **In-Situ Module Degradation Monitoring Subsystem** consists of individual loading resistors that operate the test modules at the maximum power point ($P_{max}$). Module current (I) and voltage (V) are measured simultaneously using Verivolt isolated sensors, with the total irradiance and UV radiation. sensed by the six LICORs and two TUVR sensors. The Xe lamps do not have constant output, so transient measurements of current, voltage, and irradiance are necessary to determine module $P_{max}$. Consequently, the module performance measurements are acquired at a high sampling rate (2 kHz) using three NI 9205 ADC cards.

## IV. Software Implementation

As was described in the previous section, the C-AST setup presently consists of seven main hardware subsystems, with two additional module characterization subsystems planned: *in-situ* I-V curve measurement and electroluminescence imaging.

For running a C-AST testing system, all the hardware subsystems are required to operate in parallel, coordinate with each other, and exchange data in real-time (see Figure 1).

To achieve this, the **Experiment Control and Monitoring Software** was implemented based on the *Queued State Machine–Consumer Producer Design Pattern (QSM)* [8]. This programming method allows the exchange of commands and data from multiple sources (producers), such as user events or other process, with a consumer-state machine/process that handles the commands and data in the order they were received.

Fig. 3 shows the main components of the Experiment Control Software as well as the information/data exchanged between them. Each hardware subsystem has its own dedicated queued-state machine, running in a parallel process, that controls and monitors that hardware subsystem. These hardware control-state machines receive commands and operation parameters and send back measurements to a central queued-state machine that controls and monitors the entire experiment.

In addition to the hardware control-state machines, there is a dedicated state machine for interfacing the central QSM with the experiment database that stores the experiment steps, parameters, measurements and status logs. This database QSM is also used to define new experiments and visualize and export experiment data.

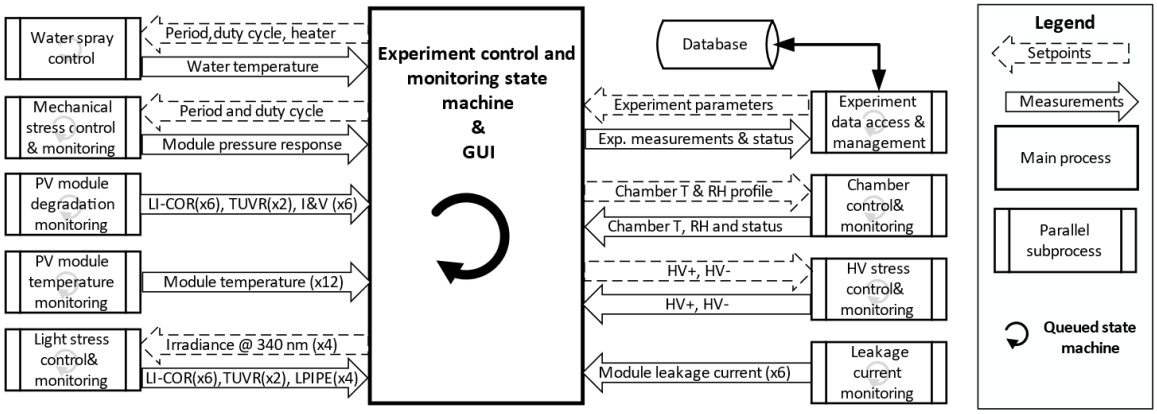


Fig. 3. Overview of software implementation.

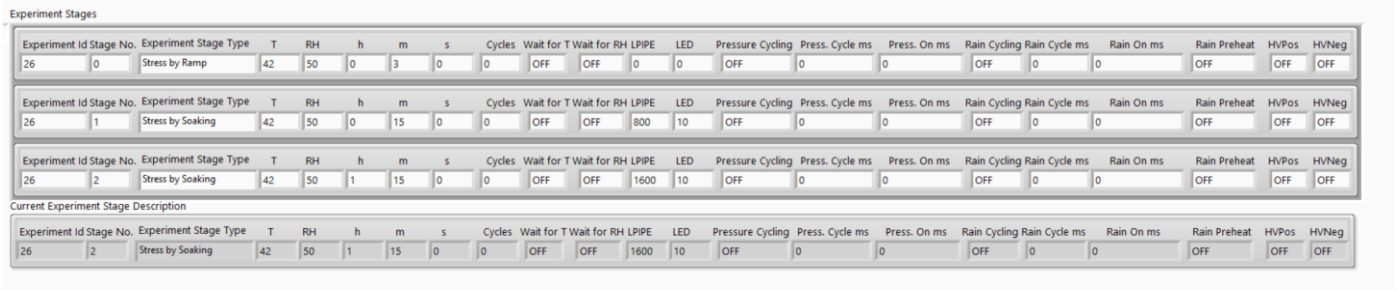


Fig. 4. Example of programming an experiment test protocol with the C-AST system.

## V. Implementation Status and Results

Currently, the hardware and software subsystems described in the above sections have been implemented, and the C-AST system is undergoing tests and calibrations. Fig. 4 shows an example of programming a test protocol with the C-AST tool.

To demonstrate the C-AST capability and develop the new C-AST protocol, a backsheet degradation study has been running since the end of January 2018. The study is performed on four-cell crystalline silicon mini-modules, undergoing the C-AST protocol shown in Table II (with ongoing optimization and calibration to the stress durations, ramps and setpoints). The results of this study will be published in a future paper [6]. However, to showcase the capabilities of the new C-AST tool, test results are shown next for a 24-h cycle.

Fig. 5 shows the environmental chamber setpoints and actual values for the air temperature and relative humidity. The module temperature (shown only for one module out of six) is ~30°C higher than air temperature during the light-stress steps of the test due to the additional absorbed heat from the lamps. The lower graph in Fig. 5 shows, in cyan, the periods of time when the water-spray cycling is enabled.

Fig. 6 shows the irradiance in the 340-nm UV band, measured with the four light-pipe photodiode sensors (LPIPE). The intensity of each of the four Xe lamps is controlled in a feedback loop based on the measured values of these LPIPE sensors, to the same reference intensity level, prescribed by the test protocol. Furthermore, Fig. 6 shows, in blue, the voltage bias applied to the module sample during the test.

The degradation of each module is monitored during the light-stress steps using loading resistors, matched for the maximum power point, and by measuring the current and voltage of each module sample. This allows one to determine the approximate module maximum power and monitor its performance degradation, as shown in Fig. 7. Moreover, leakage current is monitored for each module, which is often used as an indirect measure of module degradation due to high-voltage stress.

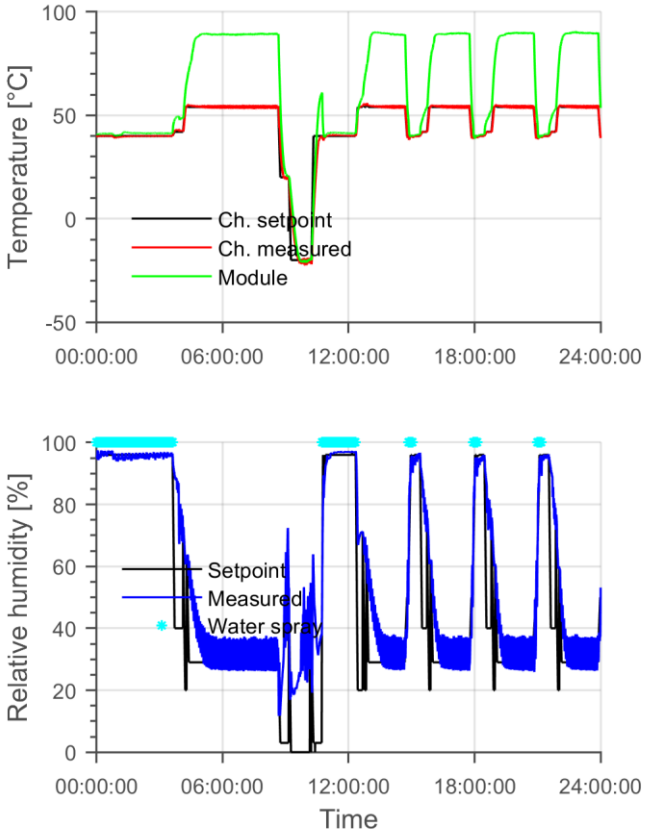


Fig. 5. C-AST protocol results (24 h, Phase b) showing: (upper) black—chamber temperature setpoint; red—measured chamber temperature; green—measured module backside temperature; and (lower) black—chamber RH setpoint; blue—measured RH; cyan—water-spray cycling on.

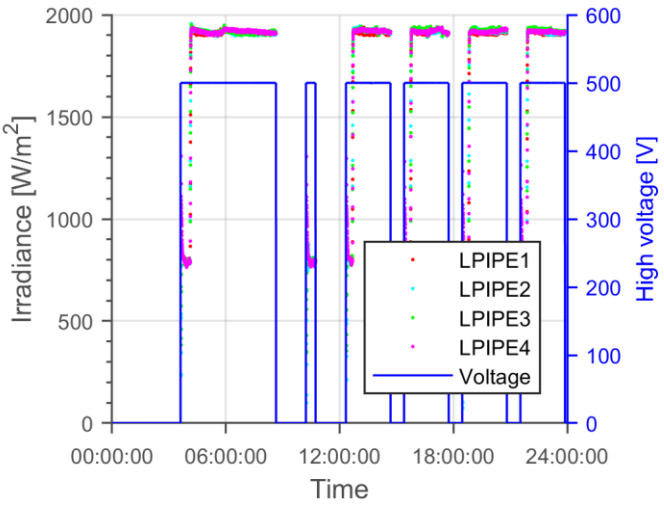


Fig. 6. C-AST protocol results (24 h, Phase b) showing the irradiance measured by the four light-pipe sensors, and the applied voltage stress for the positive-biased modules.

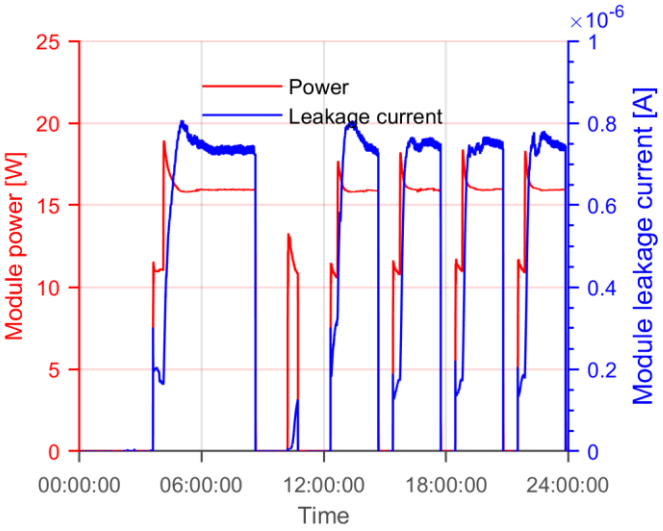


Fig. 7. C-AST protocol results (24 h, Phase b) showing: red—module power; and blue—leakage current for one of the test modules.

## VI. Discussion and Future Work

In this work, we have presented the main components and operation of a C-AST chamber, built with mostly off-the-shelf instrumentation and a standard software development tool used for instrumentation control. Such a tool can combine the environmental stress factors that have been applied sequentially or in parallel in different chambers—including light, temperature, humidity, rain/spray, system voltage, and mechanical stress (thermo-mechanical and static loading)—to reduce the number of tests, samples, and chambers required, effectively reducing the cost of testing and increasing confidence in the evaluation of PV module material and design durability.

From a capability improvement perspective, the next steps are:

- Upgrade the module leakage-current monitoring with floating-voltage Bluetooth multimeters, which would enable monitoring for high-voltage bias (1,500 V) tests.
- Upgrade the module performance monitoring with *in-situ* current-voltage curve tracing.
- Implement *in-situ* electroluminescence image monitoring of the modules.

## Acknowledgment

This work was supported in part by Aalborg University, Otto Mønsteds Fond, and the U.S. Department of Energy (DOE) under Contract No. DE-AC36-08GO28308 with Alliance for Sustainable Energy, LLC, the manager and operator of the National Renewable Energy Laboratory (NREL). NREL is a national laboratory of the DOE, Office of Energy Efficiency and Renewable Energy. Funding provided as part of the Durable Modules Materials Consortium (DuraMAT), an Energy Materials Network Consortium funded by the DOE, Office of Energy Efficiency and Renewable Energy, Solar Energy Technologies Office. The U.S. Government retains and the publisher, by accepting the article for publication, acknowledges that the U.S. Government retains a nonexclusive, paid-up, irrevocable, worldwide license to publish or reproduce the published form of this work, or allow others to do so, for U.S. Government purposes.

## References

[1] S. Kurtz, T. Sample, J. Wohlgemuth, Z. Wei, N. Bosco, J. Althaus, *et al.*, "Moving Toward Quantifying Reliability – The Next Step in a Rapidly Maturing PV Industry," in *2015 IEEE 42nd Photovoltaic Specialist Conference (PVSC)*, 2015, pp. 1–8.

[2] S. Kurtz, I. L. Repins, P. L. Hacke, D. Jordan, and M. D. Kempe, "Qualification Testing Versus Quantitative Reliability Testing of PV-Gaining Confidence in a Rapidly Changing Technology," in *33rd European Photovoltaic Solar Energy Conference and Exhibition*, Amsterdam, NL, 2017, pp. 1302–1311.

[3] S. Kurtz, "Why a Qualification Test Can NOT be Used for Lifetime Assessment and Proposal for Pathway to Standard for Lifetime Assessment," NREL (National Renewable Energy Laboratory (NREL) NREL/PR-5J00-65080, 2015.

[4] S. Kurtz, J. Wohlgemuth, M. Kempe, N. Bosco, P. Hacke, D. Jordan, *et al.*, "Photovoltaic Module Qualification Plus Testing," National Renewable Energy Laboratory, Golden, Colorado, USA NREL/TP-5200-60950, December 2013.

[5] G. TamizhMani, "Long-Term Sequential Testing (LST) of PV Modules," in *PV Module Reliability Workshop*, 2012.

[6] M. Owen-Bellini, P. Hacke, M. Kempe, D. C. Miller, S. V. Spataru, L. Schelhas, *et al.*, "Combined-Accelerated Stress Testing for Advanced Reliability Assessment of Photovoltaic Modules," in *35th EU PVSEC*, Brussels, 2018.

[7] N. Trang, H. Yushi, D. Takuya, and M. Atsushi, "Effects of UV on Power Degradation of Photovoltaic Modules in Combined Acceleration Tests," *Japanese Journal of Applied Physics,* vol. 55, p. 052301, 2016.

[8] A. Lukindo. (2007, 19 Jan). *LabVIEW Queued State Machine Producer-Consumer Architecture*. Available: http://www.mezintel.com/blog/labview-queued-state-machine/